A Tropical Influence on Global Climate

EDWIN K. SCHNEIDER

Center for Ocean–Land–Atmosphere Studies, Calverton, Maryland

RICHARD S. LINDZEN

Massachusetts Institute of Technology, Cambridge, Massachusetts

BEN P. KIRTMAN

Center for Ocean–Land–Atmosphere Studies, Calverton, Maryland

(Manuscript received 12 February 1996, in final form 28 October 1996)

ABSTRACT

A potential influence of tropical sea surface temperature on the global climate response to a doubling of the CO_2 concentration is tested using an atmospheric general circulation model coupled to a slab mixed layer ocean. The warming is significantly reduced when sea surface temperatures in the eastern equatorial Pacific cold tongue region between latitudes 2.25°N and 2.25°S are held at the control simulation values. Warming of the global mean temperature outside of the cold tongue region is reduced from 2.4°C in the unconstrained case to 1.9°C when the sea surface temperature constraint is applied. The decrease in the warming results from a positive net heat flux into the ocean cold tongue region and implicit heat storage in the subsurface ocean, induced by horizontal atmospheric heat fluxes. The reduced surface temperature warming outside of the cold tongue region is due to reduction in the downward longwave radiative flux at the surface, caused in turn by reduced atmospheric temperature and moisture. The global mean surface temperature responds to the heat storage in the ocean as if the global mean radiative forcing due to the doubled CO_2 (approximately 4 W m^{-2}) was reduced by the value of the global mean heat flux into the ocean. This mechanism also provides a possible explanation for the observed high correlation on interannual timescales between the global mean tropospheric temperature and sea surface temperature in the eastern tropical Pacific. The results emphasize the importance of correctly modeling the dynamical processes in the ocean and atmosphere that help determine the sea surface temperature in the equatorial eastern Pacific, in addition to the thermodynamical processes, in projecting global warming.

1. Introduction

The major signal in satellite measurements of global mean lower-tropospheric temperature anomalies (T_{2R}) for the past decade and a half (Christy and McNider 1994) is associated with the El Niño–Southern Oscillation (ENSO) cycle and in particular with the anomalies of sea surface temperature (SST) in the eastern equatorial Pacific. Approximately 70% of the variance of T_{2R} is explained by correlation with an ENSO index taken as the average SST in the Niño 3 and Niño 4 regions, extending from 5°S to 5°N latitudes and from 160°E to 90°W longitudes, accounting for about 3% of the earth's surface area. A similar correlation has been found between eastern equatorial Pacific SST anomalies and atmospheric temperature averaged over the Northern Hemisphere from the surface to 25 km (Pan and Oort 1983; Peixoto and Oort 1992, their Fig. 16.13).

The SST in the tropical eastern Pacific is known to be strongly affected by dynamical as well as thermodynamic interactions between the atmosphere and ocean [e.g., Bjerknes (1969) and Wyrtki (1985) for early discussions; a brief review of subsequent work can be found in Schneider et al. (1995), section 1]. In particular, changes in the surface wind stress on the ocean are extremely important in producing SST anomalies in the cold tongue region. The changes in SST lead to changes in the heat flux into the ocean and implicitly to horizontal heat fluxes in the atmosphere, which tend to damp the SST anomalies.

Both the climatology and the variability of the eastern tropical Pacific SST have proven to be very difficult to simulate correctly with current state-of-the-art coupled ocean–atmosphere general circulation models (Mechoso et al. 1995). Coupled models used in transient climate simulations require large flux corrections, especially in the eastern equatorial Pacific, to correctly simulate the

Corresponding author address: Dr. Edwin K. Schneider, Center for Ocean–Land–Atmosphere Studies, 4041 Powder Mill Road, Suite 302, Calverton, MD 20705-3106.

current climatology. For example, Murphy (1995) reports that the annual mean heat flux adjustment applied in the Hadley Centre coupled model exceeds 50 W m^{-2} over much of the eastern equatorial Pacific. We show that inaccuracies in the simulation of changes of SST in this sensitive region could lead to large errors on the global scale. Hence, it is essential for accurate predictions of the effects of increasing CO_2 that the processes that maintain the SST in the eastern tropical Pacific be correctly modeled.

The unique sensitivity of the coupled ocean–atmosphere system in the eastern equatorial Pacific SST on interannual timescales has led some investigators to suggest that dynamical coupled ocean–atmosphere processes in this region could lead to a negative feedback on global warming (Sun and Liu 1996; Clement et al. 1996). The mean zonal winds in the eastern equatorial Pacific region are easterly, and, in response, near-equatorial ocean dynamics gives a thermocline shallower in the eastern than in the western Pacific. Consequently, cold subsurface water is closer to the surface in the eastern than the western Pacific, which leads to cooler SST in the east. A strengthening of the easterlies in the equatorial Pacific would then be expected to lead to lower SST in the east.

The intensity of the hydrologic cycle in the Tropics increases in simulations of the response to increasing CO_2. If this intensification was associated with stronger surface easterlies in the eastern equatorial Pacific, as might be expected, a negative feedback mechanism could operate. The coupled negative feedback mechanism applies locally where cool subsurface waters are exposed to the surface. The locally cooler surface temperature is associated with a net increase in the heat flux into the ocean. If this increased heat flux is not balanced by reduced heat flux into the ocean elsewhere, the coupled feedback will lead to heat storage in the subsurface ocean. This negative feedback mechanism could be important in retarding warming in transient CO_2 simulations but may not be important for equilibrium climate sensitivity. On the other hand, if surface easterlies in the tropical eastern Pacific became weaker with increasing CO_2, as in the coupled model quadrupled CO_2 sensitivity experiment of Knutson and Manabe (1995) or the transient experiment of Meehl and Washington (1996), the feedback would work in the reverse direction.

We describe experiments with an atmospheric general circulation model (GCM) coupled to a slab mixed layer ocean that examine the potential effects of this local negative feedback on the global climate. The experiments suggest that the negative feedback could have important large-scale consequences and have a significant impact on warming due to increasing CO_2 concentrations. While these experiments do not demonstrate that such a feedback will occur, they emphasize the importance of accurately modeling the air–sea interactions in the equatorial eastern Pacific in order to realistically predict the evolution of global warming.

2. Experiments

The climate sensitivity was determined using an atmospheric GCM (Schneider and Kinter 1994) coupled to a slab mixed-layer ocean with a heat capacity equivalent to 50 m of water. The model is spectral with rhomboidal-15 horizontal resolution and nine levels in the vertical and includes a full suite of physical parameterizations. No sea ice occurs in the coupled model, and horizontal heat fluxes in the ocean are taken to be zero. A similar model configuration, but with sea ice, was used by Meehl and Washington (1986). A control simulation was run with the CO_2 concentration taken as 345 ppmv to be representative of current conditions. The control case was run for 32 simulated yr. A statistical equilibrium was obtained after the first few simulated years. A monthly climatology of the control model SST was determined from years 14–18 of the control simulation. The equilibrium climate with doubled CO_2 concentration (690 ppmv) was found by an analogous 22-yr model integration. The sensitivity of the global mean surface temperature to a doubling of CO_2 was found to be about 2.4°C, which is within the range of estimates from other GCMs (Mitchell et al. 1990). The comparison to the sensitivity to other models could be somewhat misleading unless it is kept in mind that this model does not have interactive sea ice and the contribution to climate sensitivity from the sea ice–albedo feedback. If sea ice were included, the sensitivity of the model would probably be higher. In the case of Meehl and Washington (1986), the sensitivity to CO_2 doubling was 3.5°C.

The potential effect of dynamical ocean–atmosphere feedbacks in the eastern equatorial Pacific on the warming was then found by calculating the equilibrium response to doubled CO_2 with SST specified as the control run climatology over a region in the eastern equatorial Pacific, but determined by the slab mixed-layer ocean model at other ocean points. The region where SST was specified not to respond to the increase in CO_2 was taken to be the Pacific east of the date line and within 2.25° latitude of the equator (i.e., at the two latitudes closest to the equator on the model Gaussian grid, 2.25°S and 2.25°N). The calculation of land surface temperature was not altered. Initial conditions for the specified SST experiment were taken from 1 January of year 19 of the unconstrained doubled CO_2 integration. The experiment was run for 12 simulated yr, which was sufficient for equilibration. This experiment will be referred to as the ''cold tongue'' case, while the unconstrained doubled CO_2 case will be referred to as the ''doubled CO_2'' case. Results are averages over the last 4 yr for the specified SST experiment, the last 11 yr of the control integration, and the last 7 yr of the unconstrained doubled CO_2 integration.

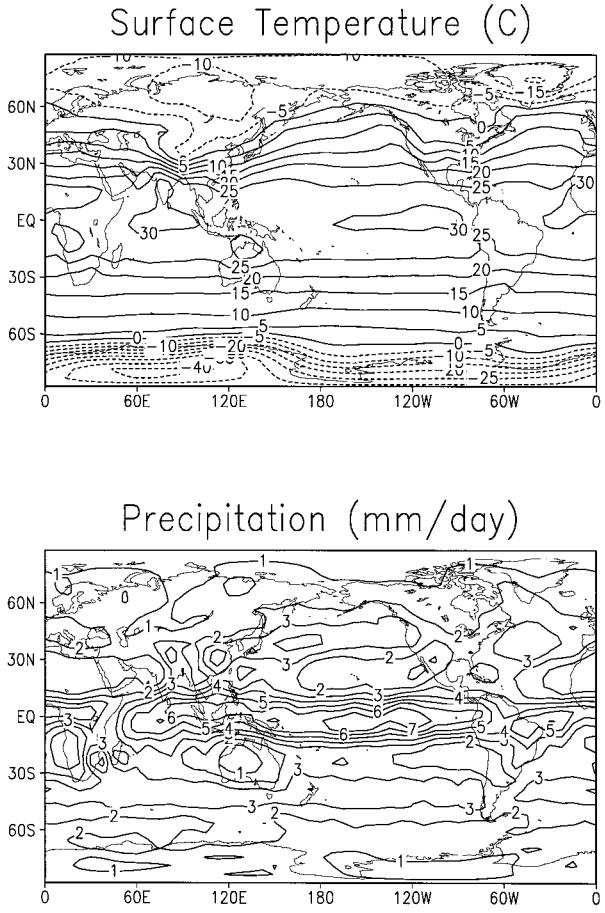

FIG. 1. Annual mean surface temperature (top, contour interval 5°C) and precipitation (bottom, contour interval 1 mm day^{-1}) for the control integration.

3. Results

The annual mean surface temperature and precipitation for the control integration are shown in Fig. 1. These results are similar to those described by Meehl and Washington (1986). Since no ocean heat fluxes are specified, these fields can be thought of as simulating the climate in the absence of oceanic heat transports. A significant difference between nature and the results shown in Fig. 1 is that the model simulation produces climatological maxima of SST and precipitation in the eastern equatorial Pacific, whereas in nature the maxima of these quantities occur in the western equatorial Pacific. To the extent that the atmospheric GCM is realistic, it can be inferred that the change from an eastern to a western equatorial Pacific warm pool then results from heat transports by the ocean circulation.[1] Similarly, the annual cycle of equatorial Pacific SST is unrealistic in the model, with a very weak annual cycle in the eastern Pacific and a much stronger annual cycle in the Pacific west of the date line. This structure is opposite to observations (e.g., Mechoso et al. 1995), and the difference is due to the neglect of ocean heat transports or regional differences in the effective heat capacity of the mixed layer in the real ocean. These unrealistic features in the model are important to keep in mind when attempting to apply the results of the experiments to the real climate system.

The change in zonal wind stress averaged over the equatorial Pacific between the unconstrained doubled CO_2 and control simulations, which would lead to dynamical response in the ocean thermocline and SST in the coupled case, was small and would be unlikely to initiate a coupled feedback, either positive or negative. Again, however, the SST and precipitation climatology of the model as shown in Fig. 1 are not realistic enough to allow any conclusions about potential coupled feedbacks in nature.

The equilibrium response in the CO_2 doubling experiments for the zonal average surface temperature, including land points, is shown in Fig. 2. The SST constraint has an influence far beyond the region of the specification. The maximum reduction in the warming in the cold tongue case relative to the doubled CO_2 case is in the equatorial band, which includes the region of specified SST, but there is some reduction at all latitudes. The zonal mean temperature warming outside of the cold tongue region was reduced in the cold tongue case by more than 0.7°C between 40°S and 40°N, and the global mean climate warming, again excluding the cold tongue region, was reduced by 22% to 1.9°C.

The spatial distribution of the difference in surface temperature between the cold tongue and doubled CO_2 experiments is shown in Fig. 3. Low-latitude land areas are markedly cooler in the cold tongue case, with maximum relative cooling of greater than 1.5°C in tropical Africa, Australia, Southeast Asia, tropical South America, and the southeastern United States. Low-latitude oceans outside of the region of specified SST are generally cooler by about 0.5°C, with differences of the smallest magnitude occurring just to the north and south of the region of specified SST. In higher latitudes the difference is less systematic, positive in sign in some regions and negative in others, although the zonal mean remains negative.

The control and doubled CO_2 cases are energetically consistent in the sense that in principle[2] the only net sources and sinks of energy are through radiative ex-

[1] By similar reasoning, ocean heat transports are not necessary to produce the relative warming of the eastern relative to the western oceans in the Northern Hemisphere midlatitudes seen in Fig. 1. This feature results from atmospheric heat transports.

[2] In fact, in the course of this investigation we have discovered that the model's land surface parameterization package (Simplified SiB) does not conserve energy when coupled to the GCM but rather produces a net sink of heat over land with a global land annual mean value of 5 W m^{-2}. The source of the error is under investigation.

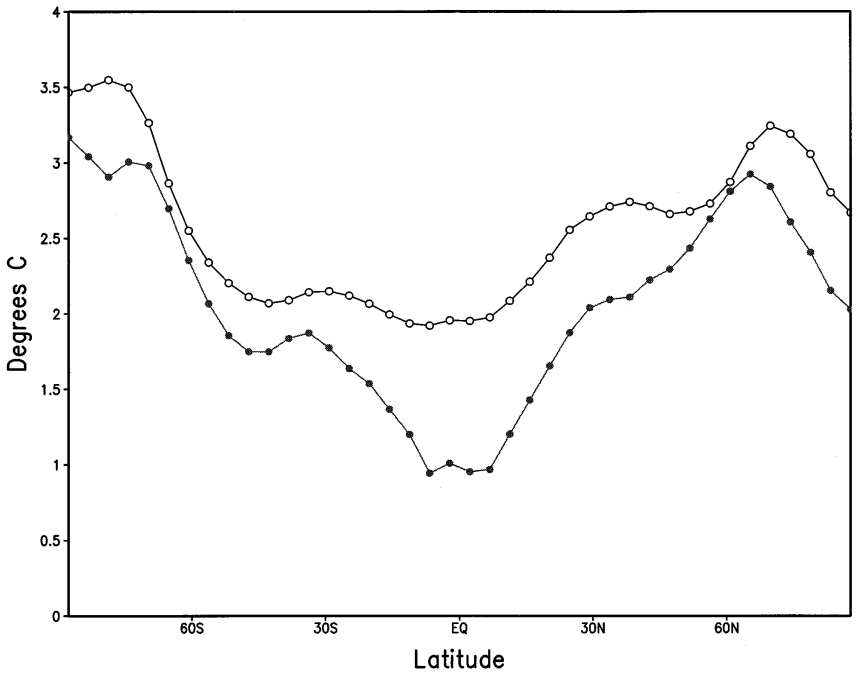

FIG 2. Difference in °C of zonal and annual mean surface temperature, doubled CO_2 minus control, for unconstrained simulation (open circles) and simulation with SST specified to have the control simulation values in the eastern equatorial Pacific (filled circles). The region of specified SST is excluded from the average in both cases.

changes at the top of the atmosphere. However, the cold tongue case is not required to satisfy this constraint in the eastern equatorial Pacific due to the specification of SST there. Consequently, in equilibrium the ocean is a net sink of energy with the imbalance in the cold tongue region reaching 70 W m^{-2} and a global mean value of 1.1 W m^{-2}. The fixed SST experiment can then be viewed as the steady-state response of the climate to a sequestration of heat in the subsurface ocean in the region of specified SST.

Large precipitation decreases are found in the cold tongue case relative to the doubled CO_2 case in the eastern tropical Pacific, but the precipitation increases over many other regions in the tropical belt (Fig. 4),

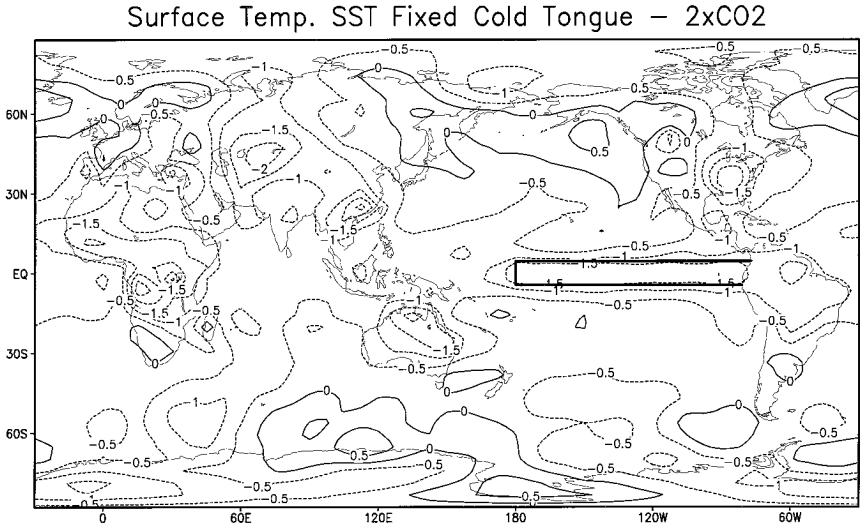

FIG. 3. Difference of annual mean surface temperature of doubled CO_2 simulation with specified SST in the eastern equatorial Pacific minus unconstrained doubled CO_2 simulation. Contour interval is 0.5°C. The area in which the SST is specified is indicated by the heavy solid line.

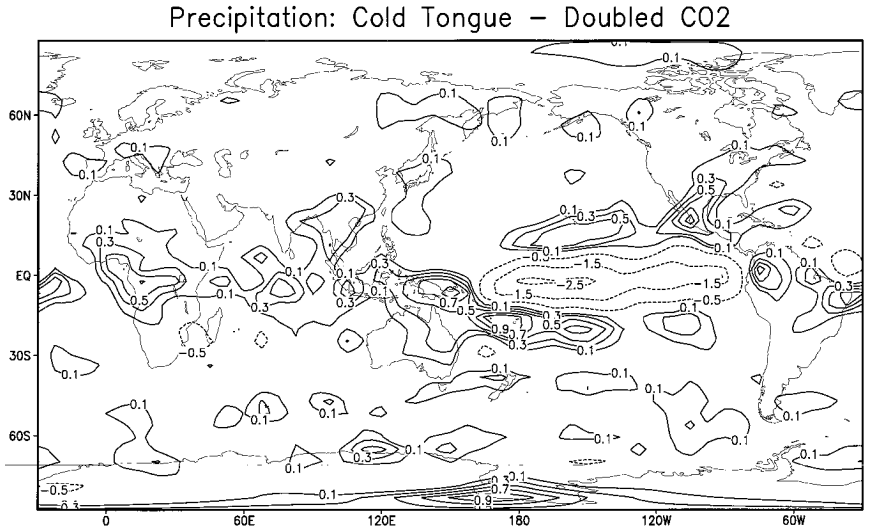

FIG. 4. Difference of annual mean precipitation of doubled CO_2 simulation with specified SST in the eastern equatorial Pacific minus unconstrained doubled CO_2 simulation in mm day^{-1}. Contour interval is 1 mm day^{-1} for negative values and 0.2 mm day^{-1} for positive values.

including land areas. The precipitation decline in the eastern equatorial Pacific dominates the global mean, which decreases by 0.07 mm day^{-1}.

Many of the features described above are similar to those observed during the La Niña, cold water in the eastern equatorial Pacific phase of the ENSO cycle. The strong signal in the global mean temperature, in phase with SST in the eastern equatorial Pacific, was noted in the introduction. Increases in the heat flux into the ocean and decreases of precipitation in the eastern equatorial Pacific, as well as increases of precipitation in the western equatorial Pacific, are observed during La Niña. The control simulation has small east–west temperature contrast across the Pacific, in effect a perpetual El Niño. The warming in the unconstrained doubled CO_2 case relative to the control simulation is practically uniform across the equatorial Pacific, varying from 2°C in the west to 1.8°C in the east. When SST in the eastern equatorial Pacific is held fixed and SST in the western equatorial Pacific is warmed, the effect is to produce a La Niña–like cooler eastern equatorial Pacific relative to the western equatorial Pacific, leading in turn to increased easterlies in the central Pacific and a shift in the maximum precipitation towards the west through mechanisms that are reasonably well understood (Gill 1980; Lindzen and Nigam 1987; DeWitt et al. 1996).

The components of the surface heat budget, as well as other model output fields, have been examined in order to understand the mechanisms by which the local SST constraint leads to these global-scale consequences. Comparison of the total surface flux forcing and the separate components in Fig. 5 shows that, in the zonal mean, the cooling of the surface temperature in the cold tongue case relative to the doubled CO_2 case is due to the decrease in the downward longwave flux at the surface. This forcing is reinforced in low latitudes by a decrease in the solar flux absorbed at the ground and partially canceled by increased solar flux in the extratropics. The latent and sensible heat fluxes in low latitudes decrease due to the decrease in the longwave forcing and change little in the extratropics. The reduction in the forcing due to the sum of these surface fluxes is balanced by cooling of the surface temperature and consequent reduced upward longwave flux at the surface. The reduction in the downward longwave radiative flux at the ground is due to reductions both in temperature throughout the troposphere and water vapor specific humidity. The reduction in water vapor amounts leads to thermal emission at the ground originating from higher and hence cooler parts of the atmosphere. These effects are largest at low latitudes (Fig. 6).

If the atmosphere–mixed layer ocean system was in local radiative–convective equilibrium outside of the region of specified SST, the atmospheric and surface temperatures differences between the doubled CO_2 and cold tongue cases would be zero except in the region of the specified SST. However, as shown in Fig. 3, the surface temperature decreases significantly over much of the globe outside of the region of specified SST. The decrease outside of the region of SST specification is then due entirely to the effect of atmospheric dynamics. A possible mechanism for the large-scale response is that dynamical constraints cause the low-latitude horizontal temperature gradients to be small (Schneider 1977, 1987). The radiative–convective equilibrium state does not satisfy these constraints, and the dynamical consequence is horizontal smoothing of the vertically averaged temperature over a much larger area than the specified SST region. The radiative imbalance at the surface in the cold tongue region leads to a global mean radi-

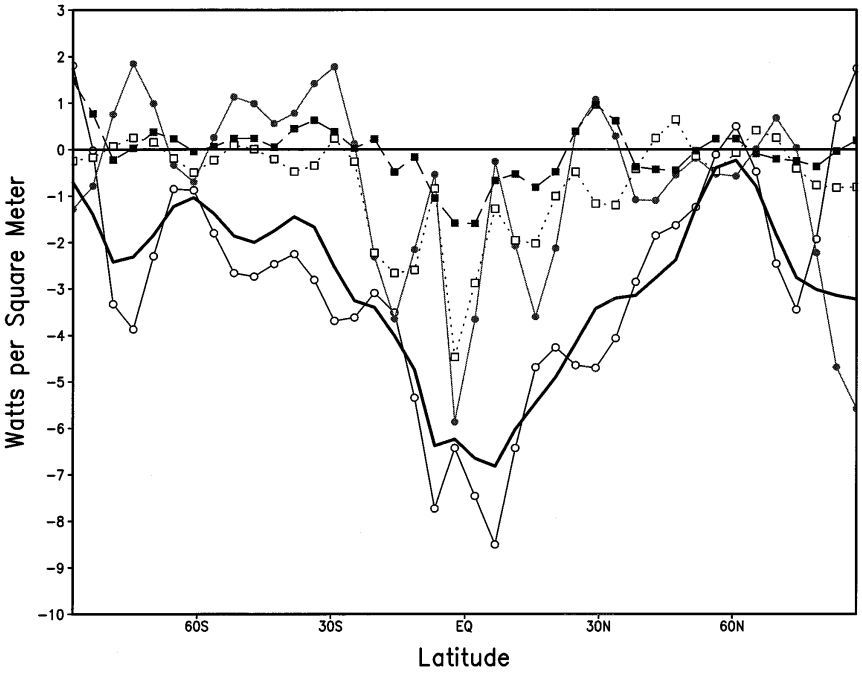

FIG. 5. Difference of zonal mean flux, cold tongue case minus doubled CO_2 case for downward longwave radiation at surface (open circles, solid line); solar flux absorbed at surface (filled circles, solid line); latent heat flux from surface (open squares, dotted line); sensible heat flux from surface (filled squares, dashed line); and total (longwave plus solar minus sensible minus latent; heavy solid line). The cold tongue region is not included in the means.

ative imbalance of 1.1 W m^{-2} into the top of the atmosphere in the cold tongue case relative to the unconstrained doubled CO_2 case. The smoothing effect of the atmospheric heat fluxes decreases atmospheric temperatures over a much larger area than the cold tongue region, spreading the outgoing longwave radiation (OLR) reduction, reducing the surface longwave forcing, and cooling the surface temperature.

The global mean increase of downward longwave radiation at the ground due to doubled CO_2 would be about 4 W m^{-2} without the water vapor feedback, which would be compensated for in equilibrium by a global mean surface temperature increase of about 1°C according to the Stefan–Boltzman law. In the GCM, the water vapor feedback amplifies the sensitivity by a factor of 2.4. The heat storage in the ocean, as seen in the radiative imbalance at the top of the atmosphere, acts to reduce the surface forcing by about 1 W m^{-2}, or by about a quarter of the global mean radiative forcing due to doubled CO_2. The 22% reduction in the global mean warming of surface temperature in the cold tongue case is then roughly consistent with the model's climate sensitivity (C. Covey 1996, personal communication).

In the simulation, the top of the atmosphere radiative imbalance required by the surface imbalance is produced by a reduction in OLR. The decrease in OLR is caused by the decreased atmospheric temperature, since the decreased specific humidity will tend to lower the effective emission level and increase the OLR. The reductions in atmospheric temperature and water vapor cooperate in decreasing the downward longwave radiation at the surface but produce effects of different sign in affecting the OLR. The temperature reduction needed to produce the required reduction in OLR is larger than that which would result without the change in specific humidity. The reduction in water vapor then produces a positive feedback in enhancing the surface temperature response, both by amplifying the decrease in atmospheric temperature and by raising the level from which longwave radiation is emitted to the surface. There appears to be no simple explanation, however, for the sign of the difference in the water vapor specific humidity shown in Fig. 6 and hence the sign of the water vapor feedback.

The zonal mean relative humidity (Fig. 6) increases by about 1%–2% above the boundary layer in the low-latitude troposphere in the cold tongue case relative to the doubled CO_2 case. This increase in relative humidity occurs despite the decrease in specific humidity and therefore results from the temperature decrease. As might naively be expected, the increase in relative humidity is associated with an increase in cloudiness and helps explain the decrease in solar flux absorbed at the ground seen in Fig. 5.

While we do not fully understand this behavior of the model relative humidity, the change diagnostically indicates that the cold tongue simulation is in a sense closer to radiative–convective equilibrium than the doubled CO_2 simulation. In the absence of large-scale mo-

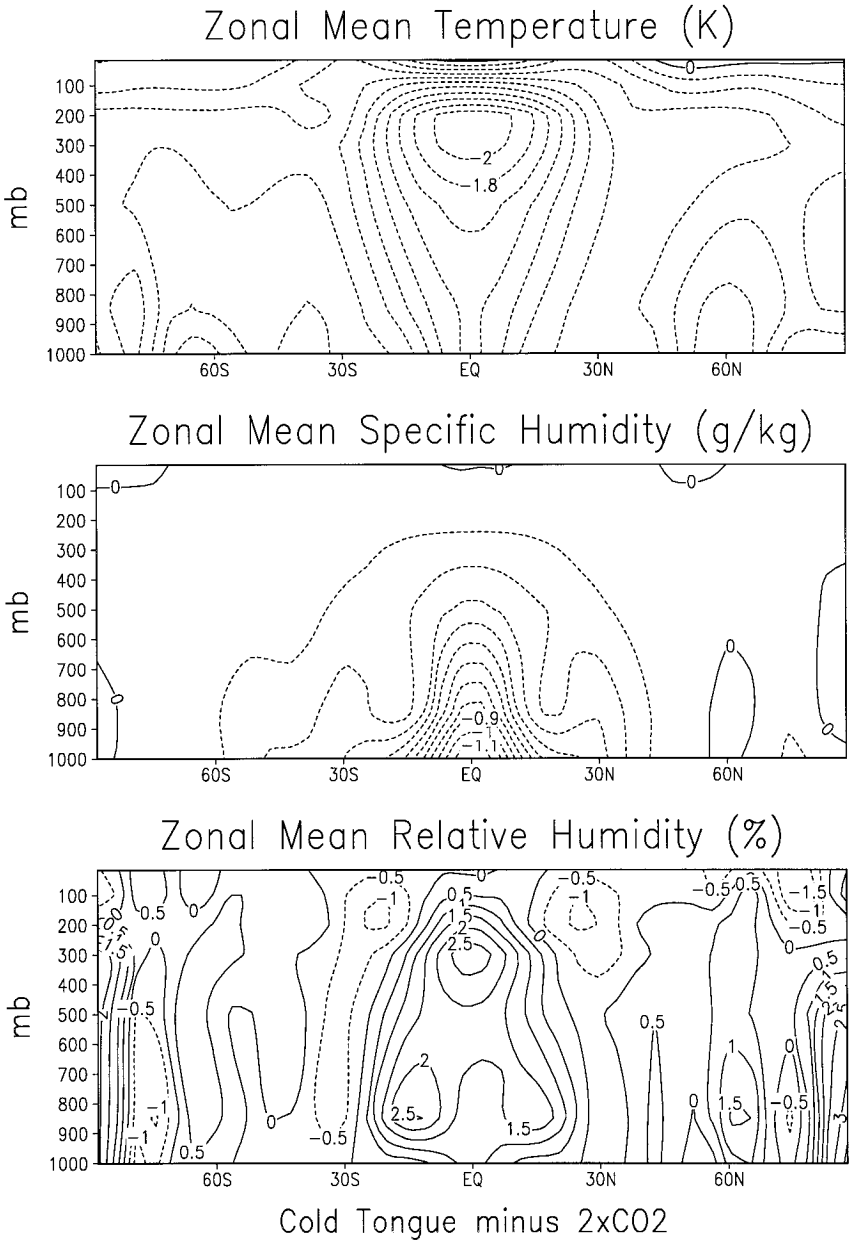

FIG. 6. Difference of zonal means as a function of latitude (*x* axis) and pressure (*z* axis, mb), cold tongue case minus doubled CO_2 case. Top: temperature difference, contour interval 0.5°K.; middle: specific humidity, contour interval 0.1 g kg^{-1}; bottom: relative humidity, contour interval 0.5%.

tions and moist convection, the atmosphere would become saturated at all heights due to vertical diffusion. In the context of the moisture budget, the subsaturation of the bulk of the atmosphere is then due to the large-scale subsidence and moist convection, by elimination. The relative roles of moist convection and the large-scale dynamics in maintaining the tropospheric water vapor distribution at subsaturation could be found by determining the GCM's radiative–convective equilibrium solution, thereby eliminating the effect of the large-scale dynamics. However, a result from Emanuel et al. (1994) makes this calculation unnecessary. That article pointed out that when the Kuo (1965) scheme is used, the atmosphere must be saturated in radiative–convective equilibrium. This argument also applies to the modified Kuo (1965) scheme used in our model, in which precipitation efficiency is related to relative humidity. Therefore both vertical diffusion and convection will tend to saturate the atmosphere at all levels. The only process in the model that reduces relative humidity in

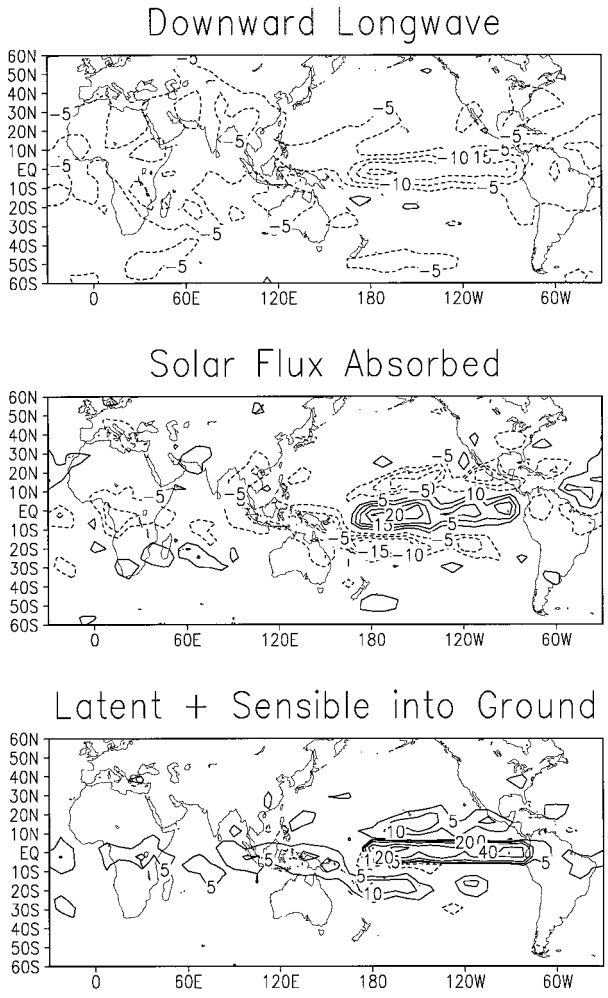

FIG. 7. Differences of heat fluxes into the ground, cold tongue case minus doubled CO_2 case. Top: downward longwave radiative flux, contour interval 5 W m^{-2}, zero contour suppressed. Middle: absorbed solar flux, contour interval 5 W m^{-2}, zero contour suppressed. Bottom: latent plus sensible heat flux into the ground, contours levels -10, -5, 5, 10, 20, 40, (60) W m^{-2}.

the tropical atmosphere is large-scale subsidence. The increase of tropical relative humidity in the cold tongue case then indicates that the drying by subsidence is reduced in importance in the moisture budget relative to the convective and diffusive moistening effects. This interpretation is consistent with the result shown in Fig. 4 that the precipitation increases practically everywhere outside the cold tongue region.

The contributions of the different surface fluxes to the local surface temperature changes between the cold tongue and doubled CO_2 cases shown in Fig. 3 have large spatial variability. These contributions are shown in Fig. 7. The largest changes are in the cold tongue region, where the cold tongue solution is not required to satisfy a local heat balance. In other regions, both ocean and land, the surface satisfies a local balance of zero net surface flux (however, see footnote two) with upward longwave flux emitted by the surface, increasing as T_s^4, where T_s is surface temperature, balancing the sum of the other fluxes. The large-scale features in the surface temperature difference are present in the difference of the downward longwave forcing. Some differences in the smaller-scale structure are associated with the other fluxes. The solar flux difference is highly correlated with the precipitation difference (Fig. 4) as is expected, since the cloud-radiative parameterization takes convective cloudiness to increase as precipitation increases. However, the relationship between cloud cover and precipitation in reality is not so clear, especially when cumulus clouds with small areal coverage are involved. There is indirect evidence that the model cloud parameterization may overemphasize the reduction of solar flux by cumulus (Schneider et al. 1997), since removing the cumulus–radiative feedback greatly improves the simulation of tropical SST in a coupled ocean–atmosphere GCM. Over land, the latent heat flux from the ground also increases with the precipitation, due to increased ground wetness. However, over land the sensible heat flux from the ground decrease is larger than the latent heat flux increase, and the net effect is an increase of latent plus sensible heat flux into the ground (i.e., a surface warming effect) in the cold tongue case. Over ocean, the sensible heat flux changes are very small and the latent heat flux changes dominate. Latent heat flux from the ocean decreases in regions of precipitation increase, possibly due to moistening of the boundary layer, leading to a surface warming tendency in the cold tongue case in the western equatorial Pacific as well as in longitudinally oriented bands on both sides of the cold tongue region. In any event, the changes in solar and latent plus sensible heat fluxes into the ground tend to cancel each other, so that surface temperature changes can be viewed as driven by the downward longwave forcing.

We have chosen the equatorial eastern Pacific as the region of specified SST because it is a region where SST is known to be very sensitive to coupled ocean–atmosphere dynamical feedbacks. We have also examined whether the structure of the surface temperature response is sensitive to the placement of the region of specified SST near the equator or near the region of most intense convection. Analogous experiments to the cold tongue case were carried out in which the SST for doubled CO_2 simulations was constrained to be that of the control simulation at all longitudes occupied by ocean in a 4.5° latitude wide strip centered off the equator. The strip was centered at 25°N in one experiment and at 25°S in another. Both of these experiments also produced significant large-scale cooling, with decreased precipitation in the hemisphere of the specified SST as well as unexpected strong precipitation increases near the equator in the opposite hemisphere. Results for the zonal mean surface temperature are shown in Fig. 8 (upper panel). The structures of the zonal mean response of the 25°S and 25°N experiments were similar, except for reflection about the equator. The model

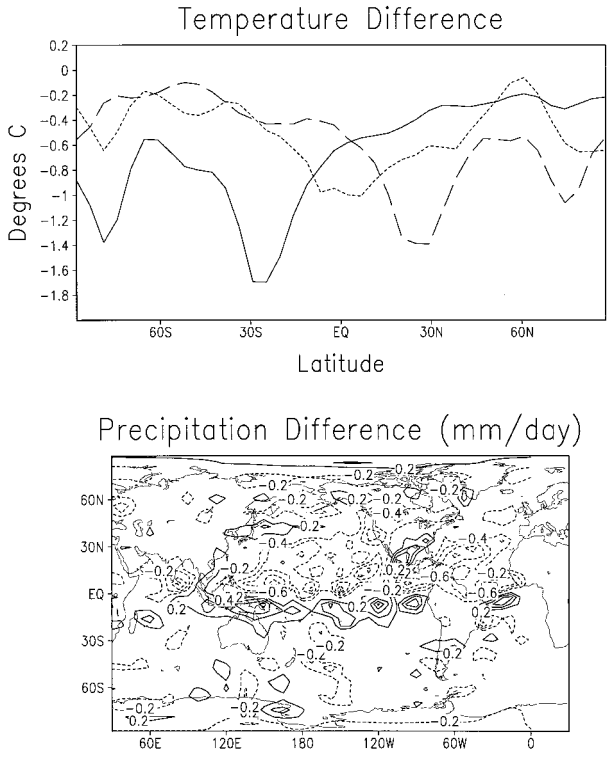

FIG. 8. Upper panel: Difference of zonal and annual mean surface temperatures, constrained SST experiment minus unconstrained doubled CO_2 simulation, for the case where SST was constrained to be that of the control simulation near 25°S (solid curve), near 25°N (long dashed curve), and in the cold tongue region (short dashed curve). The respective region of specified SST is excluded from the differences in all cases. Lower panel: Difference of annual mean precipitation for the case where SST was constrained to be that of the control simulation near 25°N minus the unconstrained doubled CO_2 simulation. Contour interval 0.2 mm day^{-1}, zero contour suppressed.

produced a maximum response near the region of specified SST, decaying away from that region with a scale similar to that for the cold tongue case. The surface temperature cooled with respect to the unconstrained doubled CO_2 case at all latitudes. Covey's climate sensitivity argument appears to explain the global mean response in the 25°N and 25°S cases, as well as in the cold tongue case, in that the reduction in warming is approximately proportionally to the area in which the SST is specified, but it is not clear that the details of the mechanism are the same in all of the cases. This linear relationship will, of course, only be true for areas of specified SST covering a small fractional area of the globe, due to the interactions between remote areas. The pronounced displacement of the ITCZ towards the hemisphere with the unconstrained SST and the reduction of precipitation in the constrained hemisphere, as shown in the lower panel of Fig. 8 for the 25°N experiment, occurred in both cases.

4. Summary

Simulations of the warming in response to doubled CO_2 with an atmospheric GCM coupled to a mixed-layer ocean have shown that artificially specifying the SST in localized regions can have a significant effect over a much larger region. These experiments show that ocean heat storage or release brought about through coupled ocean–atmosphere dynamical processes is potentially important in long-term climate projections. In the primary case considered, the SST in the equatorial eastern Pacific was taken to be the same as in the control simulation climatology. The motivations for this experiment were the observed high positive correlation between global mean atmospheric temperature and SST in the eastern tropical Pacific (Christy and McNider 1994) and the potential coupled negative feedback to global warming proposed by Sun and Liu (1996) and Clement et al. (1996). Even though this negative feedback process has not been simulated in coupled transient CO_2 simulations (e.g., Knutson and Manabe 1995), the question of the importance of coupled feedbacks in the eastern equatorial Pacific in coupled climate simulations, or even the sign of the feedback, is far from settled. Current models are inadequate to answer these questions. Coupled models produce poor simulations of the climatology of the SST, precipitation, and wind stress in the key equatorial Pacific cold tongue region (Mechoso et al. 1995), and large heat flux corrections are used to simulate the current SST climatology there.

The specification of SST produced La Niña-like conditions in the eastern equatorial Pacific relative to the unconstrained doubled CO_2 case. The warming of the global mean surface temperature, excluding the region of specification, was reduced by 22%. The reduction in warming was strongest near the equator and became smaller in high latitudes. In regions where the SST was not constrained, there was zero heat flux into the ocean in the long-term mean, but there was a large heat flux into the ocean in the region of specified SST. The decrease in warming in the specified SST integration is consistent with this heat flux into the ocean in the cold tongue region, which reached 70 W m^{-2} with a global mean of about 1.1 W m^{-2}.

Cases with SST specified near 25°N and 25°S produced significant responses in global mean surface temperature also, showing that the response is not unique to the low-latitude atmosphere. In any of the cases the local heat flux imbalance at the surface is spread over a much larger region by the atmosphere, leading to large-scale changes in the surface temperature and atmospheric circulation. However, the unique dynamics of the near-equatorial ocean suggests it likely that the cold tongue case is a more likely scenario. The surface temperature response in the cold tongue case was shown to be produced by a reduction in the downward longwave radiative flux at the ground. This reduction in the downward longwave surface forcing was caused by reductions in both the atmospheric temperature and specific humidity. On the other hand, the global mean heat imbalance at the top of the atmosphere induced by the heat storage in the ocean was satisfied by the reduction

in atmospheric temperature, with the humidity decrease acting to increase the OLR.

The ocean heat storage and atmospheric heat flux distribution mechanism discussed here could be important in the real climate system on interannual timescales. The mechanism provides a potential explanation for the high positive correlation between the global mean atmospheric temperature seen in satellite measurements and the SST in the eastern equatorial Pacific (Christy and McNider 1994). If this explanation is correct, there is a net positive heat flux into the ocean when the SST in the eastern tropical Pacific is relatively cold, and heat is stored in the ocean below the surface layers. This heat storage by itself would produce only a local cooling of the atmosphere, and little response in the atmospheric temperature elsewhere, but the atmosphere produces a heat flux that reduces horizontal temperature gradients and smooths out the temperature response, reducing temperature over a much larger area. The cooler atmospheric temperature leads to reduced downward longwave radiative flux at the ground, in response to which the surface temperatures cools. The sign of the fluxes and the differences for anomalously warm SST in the eastern tropical Pacific would be reversed. The above mechanism would not apply if the global mean surface heat flux imbalance were small or if the temperature tendency was an important term in the heat budget of the surface layer of the ocean.

The global mean surface temperature in the model responded to heat storage in the subsurface ocean as if the global mean surface radiative forcing was reduced by the value of the global mean heat flux into the ocean. That is, the model surface temperature responded to a top of the atmosphere radiative imbalance with the same sensitivity as to changes in the radiative forcing due to CO_2. If the condition of SST in approximate steady-state balance with the atmospheric forcing is met for natural climate variability, reasonable estimates of the sensitivity of the climate to changes in CO_2 could be obtained from simultaneous measurements of naturally occurring variations in the global mean surface temperature and in the top of the atmosphere radiative balance.

Acknowledgments. The research of E. K. Schneider and B. P. Kirtman was supported by NSF Grants ATM-9342469, ATM-9520579, and NOAA Grant NA26-GP0149.

R. S. Lindzen's efforts were supported by Grant 914441-ATM from the National Science Foundation. Fifteen percent of Lindzen's efforts were funded by the U.S. Department of Energy's (DOE) National Institute of Global Environmental Change (NIGEC) through the NIGEC Northeast Regional Center at Harvard University (DOE Cooperative Agreement DE-FC03-90ER61010). Financial support does not constitute an endorsement by DOE of the views expressed in this article.

We thank J. Shukla, Curt Covey, and the reviewers for useful comments.

REFERENCES

Bjerknes, J., 1969: Atmospheric teleconnections from the equatorial Pacific. *Mon. Wea. Rev.,* **97,** 163–172.

Christy, J. R., and R. T. McNider, 1994: Satellite greenhouse signal. *Nature,* **367,** 325.

Clement, A. C., R. Seager, M. A. Cane, and S. E. Zebiak, 1996: An ocean dynamical thermostat. *J. Climate,* **9,** 2190–2196.

Dewitt, D. G., E. K. Schneider, and A. D. Vernekar, 1996: Factors determining the precipitation distribution and low-level flow in the tropics of an atmospheric general circulation model: Diagnostic studies. *J. Atmos. Sci.,* **53,** 2247–2263.

Emanuel, K. A., J. D. Neelin, and C. S. Bretherton, 1994: On large-scale circulations in convecting atmospheres. *Quart. J. Roy. Meteor. Soc.,* **120,** 1111–1143.

Gill, A. E., 1980: Some simple solutions for heat-induced tropical circulations. *Quart. J. Roy. Meteor. Soc.,* **106,** 447–462.

Knutson, T. R., and S. Manabe, 1995: Time-mean response over the tropical Pacific to increased CO_2 in a coupled ocean–atmosphere model. *J. Climate,* **8,** 2181–2199.

Kuo, H. L., 1965: On the formation and intensification of tropical cyclones through latent heat release by cumulus convection. *J. Atmos. Sci.,* **22,** 40–63.

Lindzen, R. S., and S. Nigam, 1987: On the role of sea surface temperature gradients in forcing low-level winds and convergence in the tropic. *J. Atmos. Sci.,* **44,** 2418–2436.

Mechoso, C. R., and Coauthors, 1995: The seasonal cycle over the tropical Pacific in coupled ocean–atmosphere general circulation models. *Mon. Wea. Rev.,* **123,** 2825–2838.

Meehl, G. A., and W. M. Washington, 1986: Tropical response to increased CO_2 in a GCM with a simple mixed layer ocean: Similarities to an observed Pacific warm event. *Mon. Wea. Rev.,* **114,** 667–674.

——, and ——, 1996: El Niño-like climate change in a model with increased atmospheric CO_2 concentrations. *Nature,* **382,** 56–60.

Mitchell, J. F. B., S. Manabe, T. Tokioka, and V. Meleshko, 1990: Equilibrium climate change. *Climate Change: The IPCC Scientific Assessment,* J. T. Houghton, G. J. Jenkins, and J. J. Ephraums, Eds., Cambridge University Press, 131–172.

Murphy, J. M., 1995: Transient response of the Hadley Centre coupled ocean–atmosphere model to increasing carbon dioxide. Part I: Control climate and flux adjustment. *J. Climate,* **8,** 36–56.

Pan, Y.-H., and A. H. Oort, 1983: Global climate variations connected with sea surface temperature anomalies in the eastern equatorial Pacific Ocean for the 1958–1973 period. *Mon. Wea. Rev.,* **111,** 1244–1258.

Peixoto, J. P., and A. H. Oort, 1992: *Physics of Climate.* American Institute of Physics, 520 pp.

Schneider, E. K., 1977: Axially symmetric steady state models of the basic state for instability and climate studies. Part II: Nonlinear calculations. *J. Atmos. Sci.,* **34,** 280–292.

——, 1987: A simplified model of the modified Hadley circulation. *J. Atmos. Sci.,* **44,** 3311–3328.

——, and J. L. Kinter III, 1994: An examination of internally generated variability in long climate simulations. *Climate Dyn.,* **10,** 181–204.

——, B. Huang, and J. Shukla, 1995: Ocean wave dynamics and El Niño. *J. Climate,* **8,** 2415–2439.

——, Z. Zhu, B. Huang, B. S. Giese, B. P. Kirtman, J. Shukla, and J. A. Carton, 1997: Annual cycle and ENSO in a coupled ocean–atmosphere general circulation model. *Mon. Wea. Rev.,* **125,** 680–702.

Sun, D.-Z., and Z. Liu, 1996: Dynamic ocean–atmosphere coupling: A thermostat for the tropics. *Science,* **272,** 1148–1149.

Wyrtki, K., 1985: Water displacements in the Pacific and the genesis of El Niño cycles. *J. Geophys. Res.,* **90,** 7129–7132.